

Drug repurposing for coronavirus (COVID-19): in silico screening of known drugs against the SARS-CoV-2 Spike protein bound to angiotensin converting enzyme 2 (ACE2) (6M0J)

K. G. Kalamatianos

Analytical Chemistry and Toxicology Laboratory, I.Y.A., Athens, Greece

ABSTRACT

In this study FDA approved antiviral drugs and lopinavir analogues in clinical trials were tested for their inhibitory properties towards the SARS-CoV-2 Spike protein bound to angiotensin converting enzyme 2 (ACE2) (6M0J) using a virtual screening approach and computational chemistry methods. The most stable structures and the corresponding binding affinities of seventeen such antiretroviral compounds were obtained. Frontier molecular orbital theory, global reactivity descriptors, molecular docking calculations and electrostatic potential (ESP) analysis were used to hypothesize the bioactivity of these drugs against 6M0J. It is found that increased affinity for the protein is shown by inhibitors with large compound volume, small charge separation, low electrophilicity, aromatic rings and heteroatoms that participate in hydrogen bonding. Amongst the drugs tested, four compounds, PubChem CID 492005, CID 486507, CID 3010249 and lopinavir showed excellent results – binding interactions -9.0 to -9.3 kcal.mol⁻¹. These four top scoring compounds may act as lead compounds for further experimental validation, clinical trials and even for the development of more potent antiviral agents against the SARS-CoV-2.

INTRODUCTION

In December 2019 the first cases of infection from a novel coronavirus SARS-CoV-2 were reported. This new coronavirus was implicated in an outbreak of a severe pneumonia like illness COVID-19.¹⁻²

Since then COVID-19 is spreading at an alarming rate and has created an unprecedented health emergency around the globe.³⁻⁷ The virus has infected more than 23,000,000 people and 800,000 have died as of today.

There is no effective vaccine and it will most likely take at least 1-1.5 year to develop one. Therefore the development of antiviral agents is an urgent priority even though it usually takes many years for new drugs to be discovered, clinically tested and approved. A good strategy would be trying to find already approved drugs that have some efficacy against similar type of viruses.⁸ Then test the efficacy of these drugs against SARS-CoV-2 using computational chemistry methods and molecular docking.⁹⁻²¹ The most effective of these drugs can then be clinically tested and approved.

CONTACT: K.G. Kalamatianos  kgkalamatianos@gmail.com Anal. Chem. & Toxicology Lab., I.Y.A., Athens, Greece

The present work has the following objectives:

- i) to obtain the ground state optimized structures of selected antiretroviral drugs and their analogues (Tables 1–2) at a semiempirical level (PM3)²²⁻²⁵ and subsequently calculate global reactivity descriptors – softness (s), electrophilicity index (ω) - to identify differences in reactivity.
- ii) to calculate the energy gap between the highest occupied and the lowest unoccupied molecular orbital (HOMO-LUMO energy gap) of these drugs at the ground state since small energy gaps are associated with higher chemical reactivity and low kinetic stability.²⁶⁻²⁹
- iii) to investigate the interaction of the ground state optimized structure of approved antiretroviral drugs including lopinavir and its analogues (Table 2) with the SARS-CoV-2 Spike protein ([6M0J](#))³⁰ using computational chemistry methods and molecular docking.
- iv) to determine the binding affinities of these drugs (ligands) with the SARS-CoV-2 Spike protein ([6M0J](#)).

It is known that the virus enters the host cell by binding of the viral spike glycoprotein to the host receptor, angiotensin converting enzyme 2 (ACE2)³¹ therefore ([6M0J](#)) seems to be a biologically meaningful receptor.

COMPUTATIONAL METHODS

The semiempirical calculations were carried out using the Arguslab software³². Ab initio molecular orbital calculations were carried out using the ORCA 4.1 quantum chemistry program package.³³ The most stable optimized geometries and frequency calculations of the compounds studied were obtained from the PM3 method at the semiempirical level and from the PBE0/def2-SVP³⁴⁻³⁹ and the B97-3c/def2-SVP⁴⁰ methods and basis set at the ab initio level.

The recent resolved three-dimensional crystal structure of SARS-CoV-2 Spike protein bound to angiotensin converting enzyme 2 (ACE2) (PDB ID: [6M0J](#))³⁰ was retrieved from the Protein Data Bank (<https://www.rcsb.org/>) with a resolution of 2.45 Å.

Approved drugs and their analogues were downloaded from PubChem (<https://pubchem.ncbi.nlm.nih.gov/>). The most stable optimized geometries were obtained as described above and were subjected to molecular docking simulation against the SARS-CoV-2 Spike protein (PDB ID: [6M0J](#)) using the AutoDock 4.2/Autodock Vina⁴¹ softwares. The binding dissociation constant k_d and the binding free energy (ΔG_{bind}) between protein and ligand were calculated using KDEEP.⁴² The drugs were considered as ligands while the protein as macromolecule. It is well known that in computer aided drug studies, binding affinity and mode(s) of ligand with target protein can be predicted by molecular docking simulation.⁴³⁻⁴⁴

In this analysis, flexible-ligand:rigid-receptor docking was performed and accurate docking conditions were selected. All hetero atoms and water molecules were eliminated before docking. The grid box mapping parameters for AutoDock 4.2/Autodock Vina were

chosen as follows: Box dimension (Å) x= 64 y= 66 z= 72 and Center (Å) x=-23.088 y= 18.676 z= -27.106 along x, y and z directions respectively. Electrostatic potentials on molecular/vdW surfaces were computed using the Multifunctional Wavefunction Analyzer Multiwfn.⁴⁵ Pymol was used to depict protein-ligand interactions.⁴⁶

RESULTS AND DISCUSSION

The antiretroviral drugs studied in this work are listed in Table 1. Computed binding affinities of these compounds using the procedures described above are collected in Table 2. The binding affinity values (kcal.mol⁻¹) computed by AutoDock 4.2/Autodock Vina are averages of ten independent trials. The binding dissociation constants k_d and the binding free energy values (ΔG_{bind}) (kcal.mol⁻¹) were singly determined. Global reactivity descriptors of the tabulated compounds – hardness (η), softness (s), chemical potential (μ) – were calculated using the PM3 version of SCF MO and the Arguslab software.³² It may be pointed out that in SAR studies the semiempirical SCF methods are more reliable than ab initio methods.⁴⁷ The HOMO and LUMO energy values were obtained for all molecules and then the global reactivity descriptors were calculated from these values considering Koopman's theorem according to the following equations:⁴⁸⁻⁴⁹

$$\eta \approx (E_{\text{LUMO}} - E_{\text{HOMO}}) / 2 \quad (1)$$

$$s = 1 / \eta \quad (2)$$

$$\mu \approx (E_{\text{LUMO}} + E_{\text{HOMO}}) / 2 \quad (3)$$

$$\omega = \mu^2 / 2\eta \quad (4)$$

The results obtained show that best binding energies (< -8 kcal/mol) are observed in most cases for drugs that exhibit lower electrophilicity indices (electrophilicity index < 0.10) and lower to medium chemical softness s (chemical softness s < 6.4) (Table 2). The electrophilicity index ω encompasses the tendency of an electrophile to acquire an extra amount of electron density. Lopinavir and its analogues (PubChem compounds, Table 1) fall in this category. The higher binding affinity observed for these compounds can be attributed mainly to noncovalent interactions. The phenoxyacetyl amino ring is mono or disubstituted by methyl groups (-CH₃) providing high density of resonance electrons in the phenyl ring leading to higher binding affinities (Tables 1-2, Figs. 1-2). Among all sort of interactions such as CH/O, CH/N, OH/ π and NH/ π , the CH/ π is the most prominent interaction found between drugs and proteins. Docking interactions of lopinavir and an analogue compound **17** (Table 2, PubChem CID 492005) with 6M0J are shown in Figs. 1 and 2. The phenyl ring of the phenoxyacetyl amino group of lopinavir **14** interacts by forming four Pi-Alkyl interactions with VAL212, LEU91, VAL209 and PRO565. A Pi-Sigma interaction is observed between this phenyl ring and LEU95.

TABLE 1: List of antiviral agents and analogues docked against the SARS- CoV-2 spike protein 6MOJ.

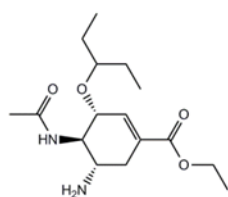
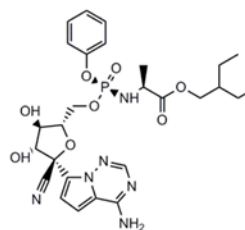
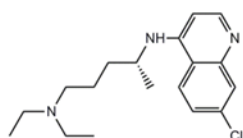
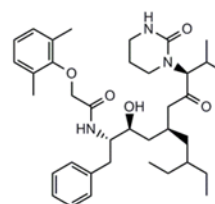
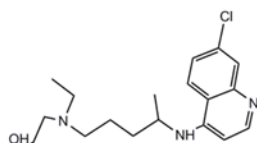
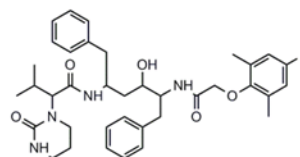
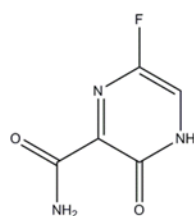
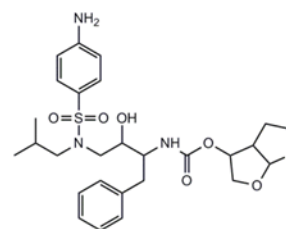
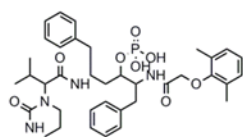
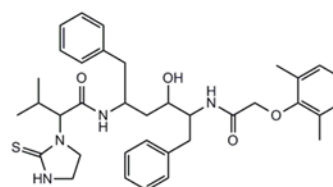
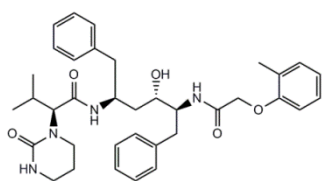
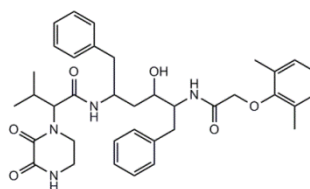
oseltamivir
1remdesivir
6chloroquine
2PubChem CID: 497932
7hydroxychloroquine
3PubChem CID: 492009
8favipiravir
4darunavir
9PubChem CID: 42637857
5PubChem CID: 3010244
10

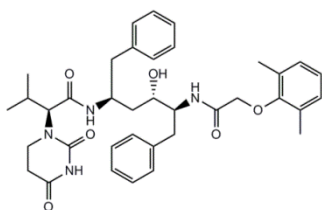
TABLE 1 (continued) : List of antiviral agents and analogues docked against the SARS- CoV-2 spike protein 6M0J.



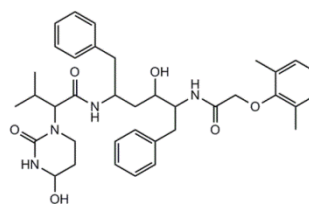
PubChem CID: 492001

11

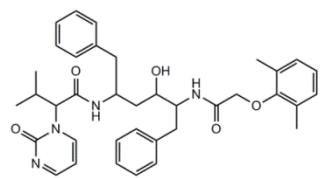
PubChem CID:3010249

15

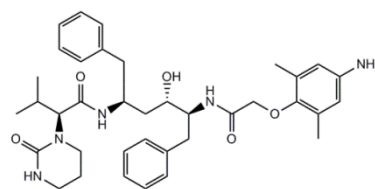
PubChem CID: 486506

12

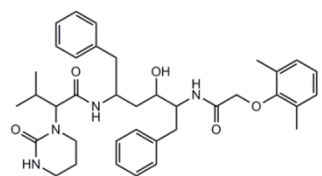
PubChem CID: 486507

16

PubChem CID: 448420

13

PubChem CID:492005

17

lopinavir

14

TABLE 2: Binding affinity data of inhibitors 1 to 17 against 6MOJ, global reactivity descriptors, Pk_d (k_d dissociation constants) and binding free energies (ΔG_{bind}).

#	Compound	HOMO - LUMO Energy Gap (a.u)	Hardness (n)	Softness (s)	Chemical Potential (μ)	Electrophilicity Index (ω)	Pk_d	ΔG_{bind}	Binding Affinity (kcal.mol^{-1})
1	oseltamivir	0.3434	0.1677	5.9633	-0.1797	0.096	2.85	-3.85	-6.5
2	chloroquine	0.2929	0.1320	7.5733	-0.1753	0.1163	3.71	-5.01	-6.6
3	hydroxychloroquine	0.2929	0.1318	7.5897	-0.1759	0.1174	3.54	-4.78	-6.8
4	favipiravir	0.3283	0.1409	7.0964	-0.2105	0.1573	4.03	-5.44	-7.0
5	PubChem CID 42637857	0.3440	0.1706	5.8603	-0.1748	0.089	3.64	-4.92	-8.1
6	remdesivir	0.2996	0.1323	7.5611	-0.1848	0.1291	3.29	-4.45	-8.1
7	PubChem CID 497932	0.3459	0.1734	5.7663	-0.1719	0.085	3.51	-4.74	-8.4

TABLE 2 (continued): Binding affinity data of inhibitors 1 to 17 against 6M0J, global reactivity descriptors, P_{k_d} (k_d dissociation constant) and binding free energies (ΔG_{bind})

#	Compound	HOMO - LUMO Energy Gap (a.u)	Hardness (n)	Softness (s)	Chemical Potential (μ)	Electrophilicity Index (ω)	P_{k_d}	ΔG_{bind}	Binding Affinity (kcal.mol ⁻¹)
8	PubChem CID 492009	0.3425	0.1681	5.9472	-0.1774	0.0936	3.53	-4.77	-8.4
9	darunavir	0.3151	0.1414	7.070	-0.1897	0.1273	4.02	-5.42	-8.5
10	PubChem CID 3010244	0.2918	0.1390	7.1948	-0.1597	0.0917	3.60	-4.85	-8.5
11	PubChem CID 492001	0.3466	0.1742	5.7402	-0.1714	0.0843	3.51	-4.74	-8.6
12	PubChem CID 486506	0.3488	0.1742	5.7410	-0.1748	0.0878	3.76	-5.08	-8.8
13	PubChem CID 448420	0.3185	0.1483	6.7424	-0.1811	0.1106	4.15	-5.60	-8.9
14	lopinavir	0.3431	0.1704	5.8674	-0.1737	0.0886	6.89	-9.31	-9.0

TABLE 2 (continued): Binding affinity data of inhibitors 1 to 17 against 6M0J, global reactivity descriptors, P_{k_d} (k_d dissociation constants) and binding free energies (ΔG_{bind})

#	Compound	HOMO - LUMO Energy Gap (a.u)	Hardness (n)	Softness (s)	Chemical Potential (μ)	Electrophilicity Index (ω)	P_{k_d}	ΔG_{bind}	Binding Affinity (kcal.mol ⁻¹)
15	PubChem CID 3010249	0.3474	0.1731	5.7763	-0.1749	0.0883	6.21	-8.38	-9.1
16	PubChem CID 486507	0.3476	0.1733	5.7695	-0.1747	0.0880	3.58	-4.84	-9.1
17	PubChem CID 492005	0.3214	0.1638	6.1035	-0.1544	0.0728	3.43	-4.63	-9.3

Significant hydrogen bonding is also observed in lopinavir **14** and its analogues (Figs. 1 and 2) that not only contributes in increasing binding affinity but may also increase binding specialty. The hydroxyl group of lopinavir interacts with GLN98 to form a hydrogen bond. The two O atoms of the phenoxyacetyl group form two H bonds with ASN210 and the –NH group one H bond with TYR196. A total of four H bonds are observed between lopinavir and 6M0J (Fig. 1). The lopinavir analogue **17** shows a total of five hydrogen bonds. The hydroxyl group interacts with ASP382 and TYR385 forming two H bonds, the –NH₂ substituent of the phenoxyacetyl group forms one hydrogen bond with ASN397, the NH group attached to the phenoxyacetyl group interacts with one H bond with ASN394 and the carbonyl oxygen close to the tetrahydro pyrimidine ring forms one H bond with ASP350 (Fig. 2).

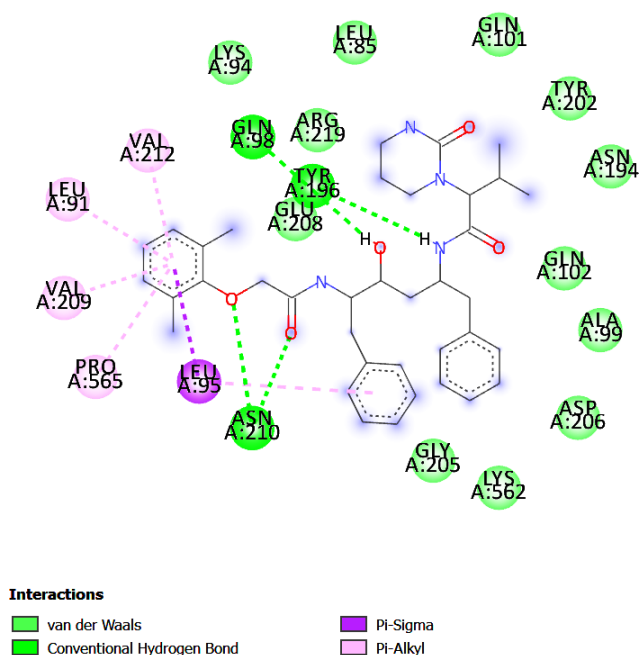


Figure 1. Docking interactions of lopinavir with 6M0J

In contrast, only three drugs that exhibit relatively higher electrophilicity indices (electrophilicity index $\approx 0.11 - 0.13$) show binding energies lower than -8 kcal/mol (< -8 kcal/mol). These compounds have also high values of chemical softness s (chemical softness $s > 6.4$) and relatively small HOMO-LUMO gaps.

These molecular orbital properties and noncovalent interactions contribute to the observed higher chemical reactivities and binding affinities respectively compared to others. Remdesivir **6**, darunavir **9** and compound **13** (PubChem CID 448420) fall in this category.

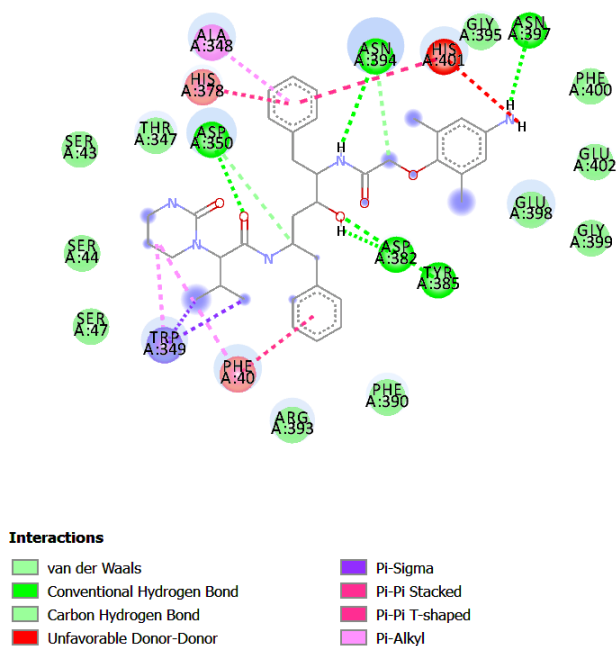


Figure 2. Docking interaction of lopinavir analogue PubChem CID492005 with 6M0J.

Remdesivir **6** interactions with 6M0J are depicted in Fig.3. Six hydrogen bonds are formed. Four of them between four oxygen atoms of **6** and ASN394, ASP350 and two of them between the H atoms of the NH₂ substituent and ALA348 and ASP382. A Pi-Cation bond is formed between the heteroatomic ring and HIS401. Two Pi-Alkyl interactions are observed between two remdesivir rings and ARG393 and ALA348 respectively and one Pi-Alkyl interaction between the CH₃ group of remdesivir and TRP349. A phenyl ring of **6** forms two Pi-Pi stacking interactions with PHE390 and PHE40. A Pi-Pi stacking interaction is also formed between the nitrogen containing ring and HIS401.

The antiretroviral drugs **1-4** show lower binding scores (binding energies > -7.1 kcal/mol) with 6M0J compared to darunavir, remdesivir, lopinavir and its analogues (compounds **9**, **6**, **5**, **7-8**, **10-17**, Table 2). These drugs also exhibit higher electrophilicity indices (electrophilicity index \approx 0.10 – 0.15). A representative binding image of oseltamivir **1** (Table 1) with 6M0J is given in Fig.4. Oseltamivir shows the lowest binding score (binding energy = -6.5 kcal/mol).

Three hydrogen bonds are formed between three oxygen atoms of **1** and LYS562, ASN210, ASN210. One carbon-hydrogen bond interaction is formed with GLU208 and two alkyl bond interactions of the ethyl groups of oseltamivir with LYS562 and LEU95.

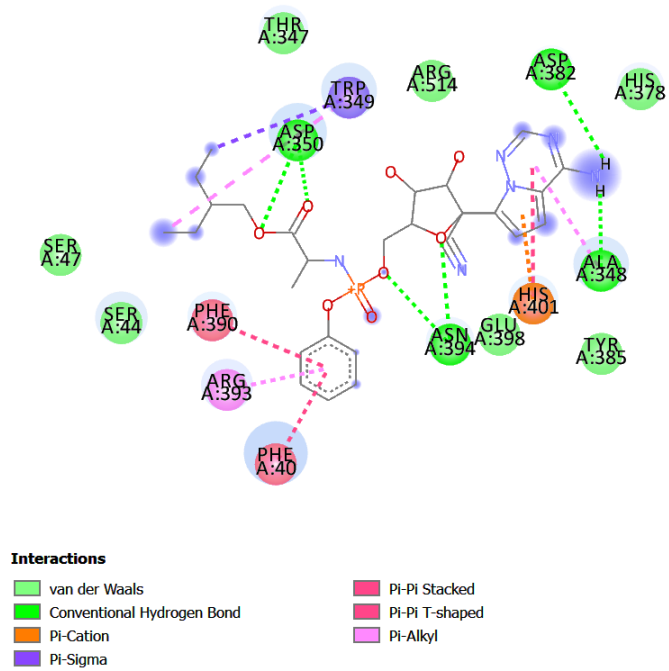


Figure 3. Docking interaction of remdesivir with 6MOJ.

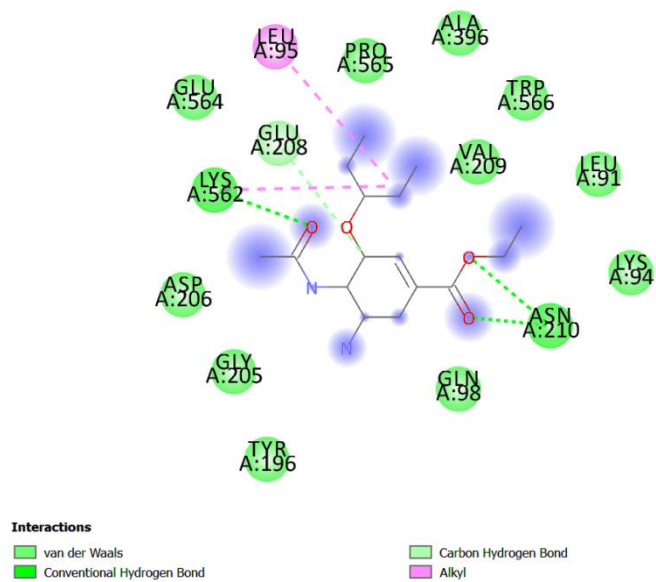


Figure 4. Docking interaction of oseltamivir with 6MOJ.

The absence of Pi-Alkyl and Pi-Pi and the small number of total interactions results to the lowest binding score with 6M0J.

Drug (ligand) interactions with 6M0J (protein) was further studied by electrostatic potential analysis on the drugs molecular surface. The value of electrostatic calculations for understanding and predicting molecular properties has been recognized for decades. It is well-known that molecular electrostatics can be predictive of a molecule's chemical reactivity and its ability to form certain types of interactions. Electrostatic potential surfaces (ESP) are used to visualize the electrostatic nature of molecules.⁵⁰⁻⁵¹ Drugs with a low and a high binding score to 6M0J, favipiravir **4** and lopinavir **14** respectively, were selected from Table 2 and their wavefunctions produced at the B97-3c/def2-SVP⁴⁰ level. The electrostatic potential on the favipiravir/vdW and lopinavir/vdW surfaces was computed using the above wavefunctions. As the final part of ESP analysis, the molecular surface area in each ESP range was calculated in order to quantitatively determine ESP distribution on the whole molecular surface.⁴⁵ The results obtained surface areas (\AA^2) and corresponding electrostatic potentials ESP (kcal.mol^{-1}) were used to plot histogram graphs of **14** and **4** (Fig. 5 and Fig. 6 respectively).

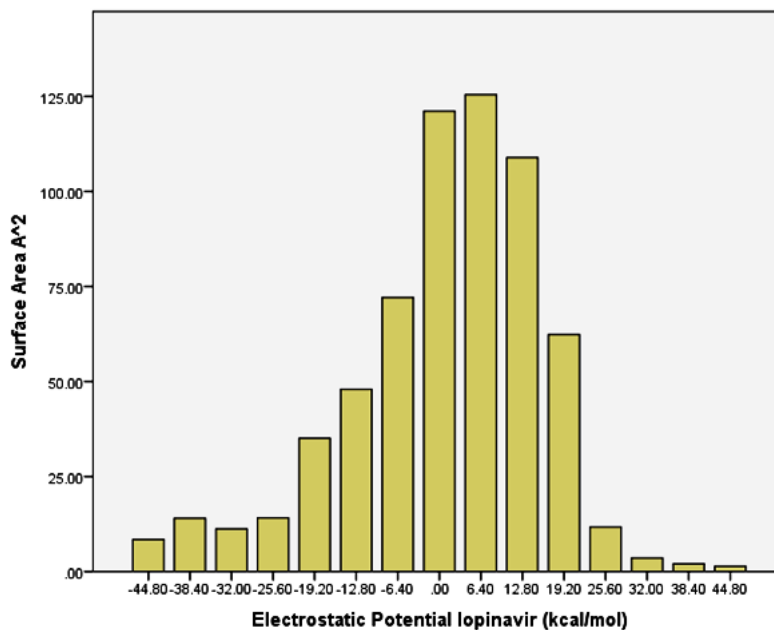


Figure 5. Surface area (\AA^2) in each electrostatic potential (ESP) (kcal.mol^{-1}) range on the vdW surface of lopinavir **14**.

From the graphs in Figs. 5 and 6 it can be seen that there is a large portion of molecular surface having low ESP values, namely from $-20 \text{ kcal.mol}^{-1}$ to 20 kcal.mol^{-1} . There are also small areas having remarkable positive and negative ESP values, corresponding to the regions closed to the global ESP minimum and maximum, respectively. These global surface maxima and minima were found to be 0.072382 au .

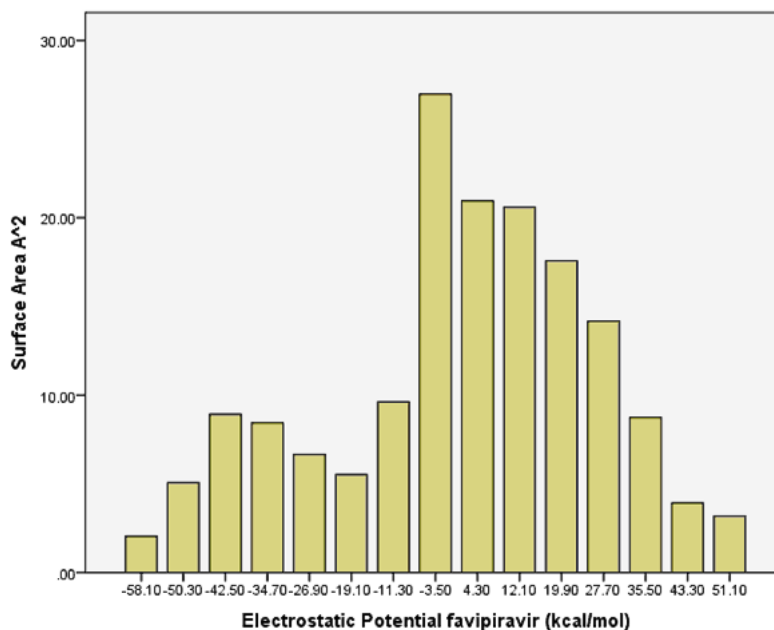


Figure 6. Surface area (\AA^2) in each electrostatic potential (ESP) (kcal.mol^{-1}) range on the vdW surface of favipiravir **4**.

($45.42068 \text{ kcal.mol}^{-1}$) and -0.072467 au. ($-45.47397 \text{ kcal.mol}^{-1}$) for lopinavir **14** and 0.085190 a.u. ($53.45785 \text{ kcal.mol}^{-1}$) and -0.098429 a.u. ($-61.76528 \text{ kcal.mol}^{-1}$) for favipiravir **4** and their observed differences suggested that the ESP distribution on the vdW surface fluctuates more remarkably in the later. Favipiravir also shows a larger internal charge separation equal to 0.0316099 a.u. ($19.83546 \text{ kcal.mol}^{-1}$) compared to 0.01821354 a.u. ($11.42918 \text{ kcal.mol}^{-1}$) of lopinavir (Table 3). This observed larger polarity of favipiravir compared to the less polar lopinavir coupled with other factors may explain the lower binding score with 6M0J.

The ESP plots of compounds **14** and **1** mapped onto the electron density surface for the ground state are shown in Fig. 7 and Fig. 8 respectively. Electron rich (negative ESP) and electron deficient areas (positive ESP) are indicated with red and white color respectively. Electron rich areas are over oxygen and nitrogen atoms and on the phenyl rings of **14** (Fig. 7) and these atoms participate in the docking interactions of this drug with 6M0J (Fig. 1). Positive potential appears over hydrogen atoms particularly to those bound with oxygen and nitrogen and this is also consistent with the reactivity shown and the hydrogen bonds formed (Fig. 1). Similarly, The ESP plot of compound **1** is very effective to predict the reactive sites of the molecule with the target protein 6M0J⁵¹ (Fig. 8 and Fig. 4). Electron rich areas appear over oxygen and nitrogen, and these atoms participate in hydrogen bonds. Electron poor areas are observed over hydrogen atoms and alkyl groups. Two alkyl bond interactions of the ethyl groups of oseltamivir **1** with LYS562 and LEU95 are formed (Fig. 4). These results demonstrate that weak inter-

TABLE 3: Surface analysis Electrostatic Potential Values (ESP) (units a.u.) computed for lopinavir 14 and favipiravir 4 using the Multiwfn Analyzer⁴⁵

ESP Values (a.u.)	Lopinavir (<u>14</u>)	Favipiravir (<u>4</u>)
Maximum Value	0.072382	0.085190
Minimum Value	-0.072467	-0.098429
Overall Average Value	0.00147382	0.00182148
Positive Average Value	0.01662140	0.03020425
Negative Average Value	-0.02122150	-0.03374761
Internal Charge Separation	0.01821354	0.03160979

actions between molecules, including H bonds and halogen bonds, can be predicted and explained by analyzing the magnitude and positions of the minima and maxima in an electrostatic potential (ESP) on the molecular vdW surface.⁵² The ESP and the drug-protein docking interaction analysis (Table 2, Figs. 1-4 and 7-8) show that for effective binding between the ligand and the receptor the main residues (aminoacids) of 6M0J (Table 4) that are involved are the TRP349, ASP350, PHE40, ASP382, ASN394, ALA348,

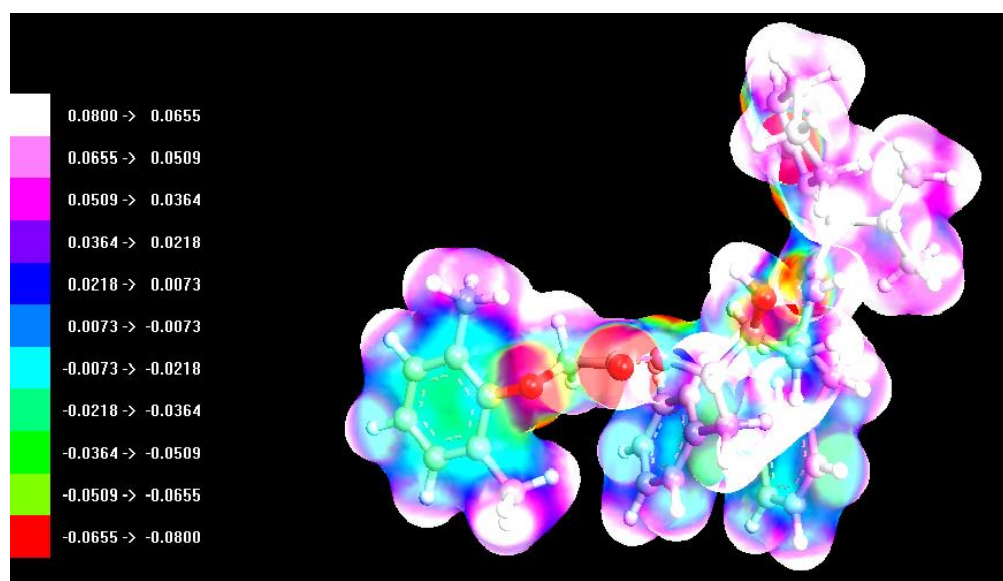


Figure 7. Electrostatic potential (ESP) mapped electron density surface of lopinavir 14 at the PM3 level

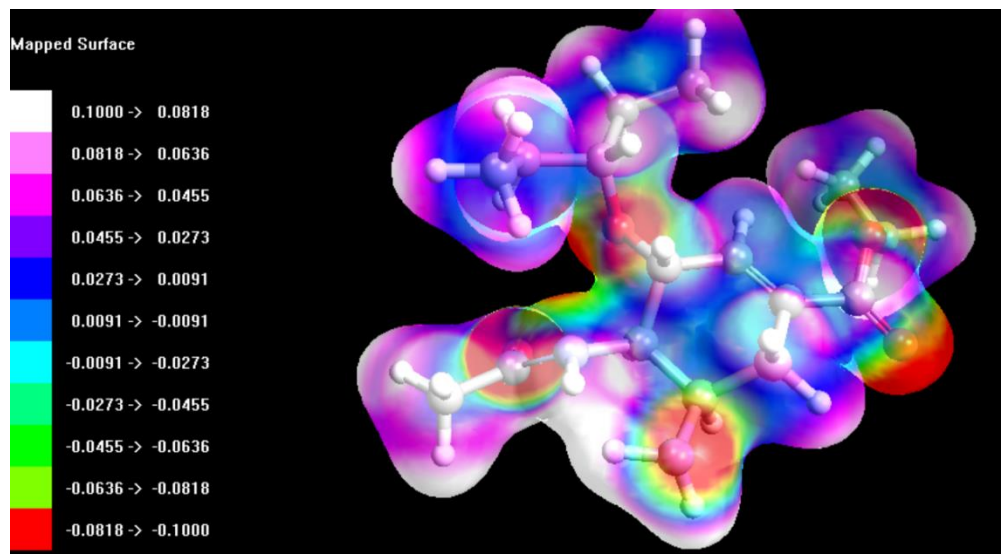


Figure 8. Electrostatic potential (ESP) mapped electron density surface of oseltamivir 1 at the PM3 level

TABLE 4: Participated main residues in protein (6M0J) - ligand (compounds in Table 2) interactions and the corresponding binding affinities (kcal.mol⁻¹).

Binding Affinities (kcal.mol ⁻¹)	Compound # (Table 2)	Main Residues of 6M0J (chain A) in contact with ligands of Table 2
< -9.1	15, 17	TRP349, ASP350, PHE40, ASP382, ASN394, ALA348, HIS378
-8.9 to -9.1	13, 14, 16	ASN210, GLN98, TYR196, LEU95, VAL212, LEU91, VAL209, PRO565
-8.6 to -8.8	11, 12	SER44, PHE 40
-8.1 to -8.5	6, 7, 8, 9	TRP349, ALA348, ASN394 PHE40, PHE390, ARG393

HIS378 or the ASN210, GLN98, TYR196, LEU95, VAL212, LEU91, VAL209, PRO565 or the SER44, PHE40 or the TRP349, ALA348, ASN394 PHE40, PHE390, ARG393 (Table 4). The formed ligand (drug in Table 2) – receptor (6M0J) complexes reveal that conventional hydrogen bonding, pi-alkyl, pi-pi stacking and halogen bonds are able to increase the binding affinity and explain the differences in binding energies. It has been reported that particularly hydrogen bonds $< 2.3 \text{ \AA}$ are able to increase the binding affinity considerably and that halogen bonds have almost similar importance as hydrogen bonds in chemical and biological systems.⁵³⁻⁵⁴

In summary, amongst the drugs of Table 2 increased affinity for 6M0J exhibit all those with large compound volume, low electrophilicity, small charge separation and with aromatic rings and heteroatoms that participate in hydrogen bonding.

Based on the binding energy, the best compounds were discovered to be the lopinavir analogues **15** – **17** (PubChem CID 486507, CID 3010249, CID 492005) and lopinavir **14**. Further optimization of these compounds can result in a more effective drug able to stop this newly emerged infection.

CONCLUSIONS

The infectious respiratory disease COVID-19 is rapidly expanding throughout the world and has become a serious threat to global health. Considering the time required to develop a vaccine or an approved drug, drug repurposing seems the most appealing, safe and straightforward approach. In this study FDA approved antiviral drugs and lopinavir analogues in clinical trials were tested for their inhibitory properties towards the COVID-19 protein (6M0J) using a virtual screening approach and computational chemistry methods. The most stable structures and the corresponding binding affinities of seventeen such antiretroviral compounds were obtained. Molecular docking calculations, ESP analysis, frontier molecular orbital theory and global reactivity descriptors were used to hypothesize the bioactivity of these drugs against the COVID-19 protein (6M0J). Compounds **5** to **13** (Table 2) showed remarkable binding interactions (-8.1 to $-8.9 \text{ kcal.mol}^{-1}$) with 6M0J. Moreover, four compounds, CID 492005, CID 486507, CID 3010249 and lopinavir (compounds **14** to **17**, Table 2) showed excellent results – binding interactions -9.0 to $-9.3 \text{ kcal.mol}^{-1}$ - for use against the newly emerged strain of coronavirus. Therefore, it is concluded that these four top scoring compounds may act as lead compounds for further experimental validation, clinical trials and for the development of more potent antiviral agents against the SARS-CoV-2.


DISCLOSURE STATEMENT

No potential conflict of interest is reported by the author.

ORCID

Konstantinos Kalamatianos  <https://orcid.org/0000-0002-0276-6531>

CONTACT

K.G. Kalamatianos  kgkalamatianos@gmail.com Analytical Chemistry & Toxicology Laboratory, I.Y.A., Athens, Greece

REFERENCES

- (1) Gorbalenya, A.E.; Baker, S.C.; Baric, R.S. et al. The species Severe acute respiratory syndrome-related coronavirus: classifying 2019-nCoV and naming it SARS-CoV-2. *Nat Microbiol*, **2020**, 5, 536–544.
- (2) Kupferschmidt, K.; Cohen, J. Will novel virus go pandemic or be contained? *Science*, **2020**, 367 (6478), 610– 611, DOI: 10.1126/science.367.6478.610.
- (3) Coronavirus Disease (COVID-2019) Situation Reports 1–45; World Health Organization, **2020**. <https://www.who.int/emergencies/diseases/novel-coronavirus-2019/situation-reports>.
- (4) Anthony, S. J.; Johnson, C. K.; Greig, D. J.; Kramer, S.; Che, X.; Wells, H.; Hicks, A. L.; Joly, D. O.; Wolfe, N. D.; Daszak, P.; Karesh, W.; Lipkin, W. I.; Morse, S. S.; Mazet, J. A. K.; Goldstein, T. Global patterns in coronavirus diversity. *Virus Evol*, **2017**, 3 (1), vex012, DOI: 10.1093/ve/vex012.
- (5) Su, S.; Wong, G.; Shi, W.; Liu, J.; Lai, A. C.K.; Zhou, J.; Liu, W.; Bi, Y.; Gao, G. F. Epidemiology, genetic recombination, and pathogenesis of coronaviruses. *Trends Microbiol.*, **2016**, 24 (6), 490– 502, DOI: 10.1016/j.tim.2016.03.
- (6) Zhu, N.; Zhang, D.; Wang, W.; Li, X.; Yang, B.; Song, J.; Zhao, X.; Huang, B.; Shi, W.; Lu, R.; Niu, P.; Zhan, F.; Ma, X.; Wang, D.; Xu, W.; Wu, G.; Gao, G. F.; Tan, W. A novel coronavirus from patients with pneumonia in China, 2019. *N. Engl. J. Med.*, **2020**, 382 (8), 727– 733, DOI: 10.1056/NEJMoa2001017.
- (7) Tang, B.; Bragazzi, N. L.; Li, Q.; Tang, S.; Xiao, Y.; Wu, J. An updated estimation of the risk of transmission of the novel coronavirus (2019-nCov). *Infect Dis Model*, **2020**, 5, 248– 255, DOI: 10.1016/j.idm.2020.02.001.

- (8) Ghosh, A.K.; Brindisi, M.; Shahabi, D.; Chapman, M.E.; Mesecar, A.D. Drug Development and Medicinal Chemistry Efforts toward SARS-Coronavirus and Covid-19 Therapeutics. *ChemMedChem.*, **2020**, *15*, 1-27, DOI:10.1002/cmdc.202000223.
- (9) Elfiky, AA. Ribavirin, Remdesivir, Sofosbuvir, Galidesivir, and Tenofovir against SARS-CoV-2 RNA dependent RNA polymerase (RdRp): A molecular docking study. *Life Sci.*, **2020**, *253*, 117592-117598, DOI: [10.1016/j.lfs.2020.117592](https://doi.org/10.1016/j.lfs.2020.117592).
- (10) Shah, B; Modi, P; Sagar, SR. In silico studies on therapeutic agents for COVID-19: Drug repurposing approach. *Life Sci.*, **2020**, *252*, 117652-117664, DOI: [10.1016/j.lfs.2020.117652](https://doi.org/10.1016/j.lfs.2020.117652).
- (11) Elfiky, AA. Anti-HCV, nucleotide inhibitors, repurposing against COVID-19. *Life Sci.*, **2020**, *248*, 117477-117483. DOI: [10.1016/j.lfs.2020.117477](https://doi.org/10.1016/j.lfs.2020.117477).
- (12) Kumar, S.; Sharma, P.P.; Shankar, U; Kumar, D.; Joshi, S.K; Pena, L.; Durvasula, R.; Kumar, A.; Kempaiah, P.; Poonam; Rathi, B. Discovery of New Hydroxyethylamine Analogs against 3CLpro Protein Target of SARS-CoV-2: Molecular Docking, Molecular Dynamics Simulation, and Structure–Activity Relationship Studies. *J. Chem. Inf. Model.*, **2020**, DOI: [10.1021/acs.jcim.0c00326](https://doi.org/10.1021/acs.jcim.0c00326)
- (13) Elmezayen, A.D; Al-Obaidi, A.; Şahin, A.T.; Yelekçi K. Drug repurposing for coronavirus (COVID-19): in silico screening of known drugs against coronavirus 3CL hydrolase and protease enzymes. *J. Biomol Struct. Dyn.*, **2020**, 1-13. DOI: [10.1080/07391102.2020.1758791](https://doi.org/10.1080/07391102.2020.1758791)
- (14) Asai, A.; Konno, M.; Ozaki, M.; Otsuka, C.; Vecchione, A.; Arai, T.; Kitagawa, T.; Ofusa, K.; Yabumoto, M.; Hirotsu, T.; Taniguchi, M.; Eguchi, H.; Doki, Y.; Ishii, H. COVID-19 Drug Discovery Using Intensive Approaches. *Int. J. Mol. Sci.*, **2020**, *21*, 2839-2848, DOI: [10.3390/ijms21082839](https://doi.org/10.3390/ijms21082839)
- (15) Rohit, B; Raj, K.N; Ravindra K. R. Drug Repurposing: A Promising Tool in Drug Discovery Against Cov-19. *Biomed. J. Sci. & Tech. Res.*, **2020**, *28*(5), 21913-21915, DOI: [10.26717/BJSTR.2020.28.004702](https://doi.org/10.26717/BJSTR.2020.28.004702).
- (16) Wang J. Fast Identification of Possible Drug Treatment of Coronavirus Disease-19 (COVID-19) through Computational Drug Repurposing Study. *J. Chem. Inf. Model.* **2020**; *60*, 3277-3286. DOI: [10.1021/acs.jcim.0c00179](https://doi.org/10.1021/acs.jcim.0c00179)
- (17) Pant S, Singh M, Ravichandiran V, Murty USN, Srivastava HK. Peptide-like and small-molecule inhibitors against Covid-19. *J Biomol. Struct. Dyn.*, **2020**, 1-10. DOI: [10.1080/07391102.2020.1757510](https://doi.org/10.1080/07391102.2020.1757510)
- (18) Joshi S, Joshi M, Degani MS. Tackling SARS-CoV-2: proposed targets and repurposed drugs. *Future Med Chem.*, **2020**, DOI: [10.4155/fmc-2020-0147](https://doi.org/10.4155/fmc-2020-0147).
- (19) Adebambo, K. Computational Investigation of the Interaction of Anti-Influenza Drugs with CoVID-19 Protein. *Computational Molecular Bioscience*, **2020**, *10*, 45-60.
- (20) Sharp, Kumar; Dange, Dr. Shubhangi In-Silico FDA-Approved Drug Repurposing to Find the Possible Treatment of Coronavirus Disease-19 (COVID-19), **2020**, ChemRxiv. Preprint. <https://doi.org/10.26434/chemrxiv.12340718.v1>
- (21) Rajbhar, Priyanka; Singh, Dikshant; Yadav, Ruchi Repurposing of SARS Inhibitors Against COVID19, **2020**, ChemRxiv. Preprint. <https://doi.org/10.26434/chemrxiv.12155361.v1>

- (22) Stewart, J.J.P. Optimization of parameters for semiempirical methods I. Method. J. Comput. Chem. **1989**, 10, 209-220, DOI: [10.1002/jcc.540100208](https://doi.org/10.1002/jcc.540100208).
- (23) Stewart, J.J.P. Optimization of parameters for semiempirical methods II. Applications. J. Comput. Chem., **1989**, 10, 221-264. DOI: [10.1002/jcc.540100209](https://doi.org/10.1002/jcc.540100209).
- (24) Stewart, J.J.P. Optimization of parameters for semiempirical methods. III Extension of PM3 to Be, Mg, Zn, Ga, Ge, As, Se, Cd, In, Sn, Sb, Te, Hg, Tl, Pb, and Bi. J. Comput. Chem. **1991** 12, 320-341. DOI: [10.1002/jcc.540120306](https://doi.org/10.1002/jcc.540120306).
- (25) Stewart, J.J.P. Optimization of parameters for semiempirical methods IV: extension of MNDO, AM1, and PM3 to more main group elements. J Mol Model **10**, **2004** 155–164 DOI: 10.1007/s00894-004-0183-z.
- (26) Sinha, L.; Prasad, O.; Narayan, V.; Shukla, SR. Raman, FT-IR spectroscopic analysis and first-order hyperpolarisability of 3-benzoyl5-chlorouracil by first principles. J Mol. Simul. **2011**, 37, 153-163.
- (27) Lewis, D.F.V.; Loannides, C.; Parke, D.V. Interaction of a series of nitriles with the alcohol-inducible isoform of P450: Computer analysis of structure-activity relationships. Xenobiotica. **1994**, 24, 401-408.
- (28) Kosar, B.; Albayrak, C. Spectroscopic investigations and quantum chemical computational study of (E)-4-methoxy-2-[(ptolyimino)methyl]phenol. Spectrochim Acta. **2011**, 78, 160-167.
- (29) Fukui, K. Role of frontier orbitals in chemical reactions. Science. **1982**, 218, 747-754.
- (30) Lan, J; Ge J; Yu, J; Shan, S; Zhou, H; Fan, S; Zhang, Q; Shi, X; Wang, Q; Zhang, L; Wang, X. Structure of the SARS-CoV-2 spike receptor-binding domain bound to the ACE2 receptor. Nature. **2020** 581, 215-220 DOI:10.1038/s41586-020-2180-5
- (31) Du, L.; He, Y.; Zhou, Y.; Liu, S.; Zheng, B.-J.; Jiang, S. The spike protein of SARS-CoV – A target for vaccine and therapeutic development. Nat. Rev. Microbiol. 2009, 7 (3), 226-236
- (32) Thompson, M.A. "Molecular docking using ArgusLab, an efficient shape-based search algorithm and AScore scoring function," in Proceedings of the ACS Meeting, Philadelphia, Pa, USA, March-April 2004, 172, CINF 42.
- (33) Neese, F. The Orca program system. Comput. Mol. Sci., **2012**, 2, Issue 1, 73-78.
- (34) Adamo, C.; Barone, V. Toward reliable density functional methods without adjustable parameters: The PBE0 model. J. Chem. Phys., **1999**, 110, 6158-6170.
- (35) Perdew, J.P.; Ernzerhof, M.; Burke, K. Rationale for mixing exact exchange with density functional approximations. J.Chem. Phys., **1996**, 105, 9982-9985.
- (36) Perdew, J.P.; Burke, K.; Ernzerhof M. Generalized Gradient Approximation Made Simple. Physical Review Letters, **1996**, 77 (18), 3865-3868.
- (37) Guido, C. A.; Brémond, E.; Adamo, C.; Cortona, P. Communication: One third: A new recipe for the PBE0 paradigm. J. Chem. Phys., **2013**, 138, 021104.
- (38) Zheng, J.; Xu, X.; Truhlar, D.G. Minimally augmented Karlsruhe basis sets. Theor. Chem. Acc., **2011**, 128, 295–305.

- (39) Stoychev, G. L.; Auer, A. A.; Neese, Frank. Automatic Generation of Auxiliary Basis Sets. *J. Phys. Chem. A*, **2017**, 121, 4379-4387.
- (40) Brandenburg, J.G.; Bannwarth, C.; Hansen, A.; Grimme S. B97-3c: A revised low-cost variant of the B97-D density functional method. *J. Chem. Phys.* **2018**;148(6):064104. DOI: 10.1063/1.5012601.
- (41) Trott, O.; Olson, A. J. Software news and update AutoDockVina: Improving the speed and accuracy of docking with a new scoring function, efficient optimization, and multithreading. *Journal of Comput. Chem.*, **2009**, 31(2), NA-461. <https://doi.org/10.1002/jcc.21334>.
- (42) Jiménez, J.; Škalič, M.; Martínez-Rosell G., De Fabritiis, G. KDEEP: Protein–Ligand Absolute Binding Affinity Prediction via 3D-Convolutional Neural Networks. *Journal of Chemical Information and Modeling* **2018** 58 (2), 287-296 DOI: 10.1021/acs.jcim.7b00650
- (43) Seeliger, D; De Groot B.L. (2010) Conformational transitions upon ligand binding: holo-structure prediction from apo conformations. *PLoS Computational Biology*, **2010**, 6: e1000634
- (44) Morris, GM; Lim-Wilby, M. (2008) Molecular Docking. In: Kukol A (Eds.). *Molecular Modeling of Proteins*. Humana Press, Totowa, NJ, pp. 365-382.
- (45) Tian, L; Feiwu C. Multiwfn – A Multifunctional Wavefunction Analyzer. *J. Comput. Chem.*, **2012**, 33, 580-592
- (46) The PyMOL Molecular Graphics System, Version 2.0 Schrödinger, LLC.
- (47) Karelson, M. *Molecular Descriptors in QSAR/QSPR*, Wiley-Interscience, New York , **2000**.
- (48) Scrocco, E; Tomasi, J. The Electrostatic Molecular Potential as a Tool for the Interpretation of Molecular Properties. In *New Concepts II*, Springer, Berlin, 1973, 42, 95-170.
- (49) Petrolongo, C. Quantum Chemical Study of Isolated and Interacting Molecules with Biological Activity. *Gazz. Chim. Ital.*, **1978**, 108, 445-478.
- (50) Weiner, P.K.; Langridge, R.; Blaney, J.M.; Schaefer, R.; Kollman, P.A. Electrostatic Potential Molecular Surfaces. *Proc. Natl. Acad. Sci.*, **1982**, 79 (12), 3754-3758.
- (51) Okulik, N.; Jubert, A.H. Theoretical study on the structure and reactive sites of non-steroidal anti-inflammatory drugs. *J. Mol. Struct. THEOCHEM*, **2004**, 682, 55-59.
- (52) Tian, X; Liu, Y; Zhu, J; Yu, Z; Han, J; Wang, Y; Hang W. Probing inhibition mechanisms of adenosine deaminase using molecular dynamics simulations. *PLoS ONE*, **2018**, 13 (11), 1-21.
- (53) Wade, R.C.; Goodford, P.J. The role of hydrogen-bonds in drug binding. *Prog. Clin. Biol. Res.*, **1989**, 289, 433-444.
- (54) Sarwar, M.G.; Ajami, D.; Theodorakopoulos, G.; Petsalakis, I.D.; Rebek, J. Amplified Halogen Bonding in a Small Space, *J.A.C.S*, **2013**, 135, 13672-13675.